STRUCTURE, PROCESSING, AND PROPERTIES OF ODS SUPERALLOYS

R. F. Singer*) and E. Arzt**)
*) BBC Brown Boveri & Company, Ltd.
5401 Baden
Switzerland
**)Max-Planck-Institut für Metallforschung
Seestrasse 92
7000 Stuttgart 1
W.Germany

ABSTRACT. The present paper reviews the technology and science of oxide-dispersion strengthened (ODS) superalloys in the light of the latest developments in COST 501 and elsewhere. The emphasis is on the alloys Inconel MA 6000 and Incoloy MA 956, on which most recent work has been performed. The essential microstructural elements in these alloys are described and illustrated. The processing steps, including mechanical alloying, powder consolidation, recrystallization, forging, joining and machining are critically examined. Further, the properties of ODS superalloys - i.e. yield, creep, fatigue and thermal fatigue strength as well as hot corrosion resistance - are reviewed and, wherever possible, compared to those of conventional superalloys. Important property improvements over the dispersoid-free counterparts are identified and the beneficial effects of the oxide dispersoids are discussed on the basis of the latest scientific progress in this area. Finally, the scope for further development of ODS alloys with regard to alloy composition, structure, and fabricability is outlined.

1. INTRODUCTION

Oxide dispersion strengthened (ODS) superalloys are advanced high temperature materials which can retain useful strength up to a relatively high fraction of their melting point. This advantage of ODS alloys over conventional superalloys is due to fine, uniformly dispersed, stable oxide particles which act as barriers to dislocation motion.

ODS superalloys are being used already in considerable quantities. The combined production of the two existing manufacturers, Sherritt-Gordon and Inco, probably surpasses 200 t/year. The alloy which is presently produced in the largest quantities is MA 754, Table 1. It has been in production use by General Electric as a vane material for the F 404 engine since 1980 /1/. DS-Ni, which ranks second in production volume, is utilized for combustor components in AVCO'S M 1 tank AGT 1500

turbine engine and Pratt & Whitney's JT 9 D engine /2/. MA 956 is a third alloy which is used commercially. Its breakthrough came in 1985 with a successful application in combustion engines.

The commercial ODS superalloys exhibit rather lean Ni-, NiCr-, or Fe-matrices as apparent from Table 1. Such alloys are easier to process but they lack oxidation and corrosion resistance. Their strength is also limited because solid solution strengthening and precipitation strengthening are not or not fully exploited. In order to overcome these problems, Inco developed the alloy MA 6000 /3-5/ which is presently being evaluated by several turbine engine manufacturers.

Alloy	Cr	Mo	W	Al	Ti	Ta	B	Zr	C	Fe	Ni	Others	Dispersoid	Status*	Producer
DS-Ni	—	—	—	—	—	—	—	—	—	—	Bal.	—	2.0 ThO_2	c	Sherritt-Gordon
MA 754	20	—	—	0.3	0.5	—	—	—	0.05	1.0	Bal.	—	0.6 Y_2O_3	c	Inco
MA 956	20	—	—	4.5	0.5	—	—	—	—	Bal.	—	—	0.5 Y_2O_3	c	Inco
MA 6000	15	2.0	4.0	4.5	2.5	2.0	0.01	0.15	0.05	1.0	Bal.	—	1.1 Y_2O_3	e	Inco
Alloy 61	9	3.4	6.6	8.5	—	—	0.01	0.15	0.05	1.0	Bal.	—	1.1 Y_2O_3	e	Inco
Alloy 49	11	1.7	6.4	7.3	—	3.2	0.01	0.15	0.05	1.0	Bal.	1.6 Nb	1.1 Y_2O_3	e	Inco
TMO-2	6	2.0	12.4	4.2	0.8	4.7	0.01	0.05	0.05	—	Bal.	9.7 Co	1.1 Y_2O_3	e	NRIM

*) c, commercial; e, experimental

Table 1: Composition (wt.%) of ODS superalloys

More recently, attempts were made by Inco to develop ODS nickel-base superalloys with very high volume fractions of gamma' (80%) /6/ /7/. Alloy 49 evolved from this program as the strongest alloy but with certain deficiencies in recrystallization behavior. It was, therefore, replaced later by Alloy 51 with better recrystallization response but somewhat lower strength.

There is also an ongoing alloy development program in Japan /8/. The only alloy known to have emerged from this program so far is alloy TMO-2. It is reported to have strength superior to MA 6000, corrosion resistance, however, is probably lower.

The purpose of the present paper is to review recent work on processing and properties of ODS superalloys. The emphasis will be on the alloys MA 6000 and MA 956, on which most of the more recent work has been performed. Attempts were made to include the work done within the framework of COST 501 - as far as the cooperating partners were willing to release that information. In this collaborative program, 24 European companies and research organizations have worked together over the last three years in order to improve the knowledge of processing and properties of MA 6000 and MA 956. For more information on ODS superalloys in general the reader is referred to some recent publications on the subject /9,10/.

2. STRUCTURE OF ODS SUPERALLOYS

The microstructure of ODS superalloys contains several characteristic features which distinguish them favourably from conventional alloys, on the one hand, but also reflect the powder metallurgical processing route in the form of less desirable microstructural constituents, on the other hand. The structural details which are characteristic for state of the art processing, will be described in the following section.

2.1. Oxide Dispersoids

MA 6000 and MA 956 contain about 2.5 and 3 volume percent, respectively, of a fine dispersion of yttrium oxide, which is incorporated in the material by the mechanical alloying process (see section 3.1.). In MA 6000, the dispersoid imparts high-temperature strength which superimposes on that contributed by gamma' precipitates, thereby extending the useful strength of the alloy to well above 1000°C.

The oxide dispersoids are nearly spherical (Fig.1 /11/) and have a mean diameter of about 30 nm. The average spacing is approximately 100 nm. On the level of TEM analysis, the desired uniformity of the dispersoid distribution is confirmed. For MA 956, similar dispersion parameters have been stated /12,13/.

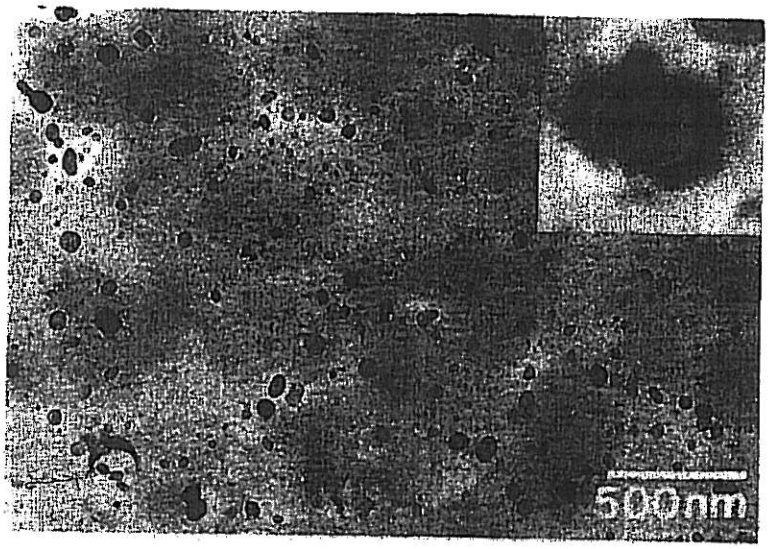

Fig. 1: TEM micrograph showing oxide dispersoids in MA 6000 (main figure) and strain contrast produced by misfitting dispersoid (insert, at 15 times higher magnification) /11/

Yttria is one of the oxides with the highest negative free enthalpy of formation, attesting to its thermal stability, and consequently only negligible dispersoid coarsening occurs in MA 6000 during exposure

to temperatures below 1000°C for even more than 10.000 h /14/. Above 1100°C, however, considerable coarsening has been observed in MA 6000 and MA 956 /15/, but it is still controversial as to whether the increase in dispersoid diameter is due to the dissolution of small dispersoids ("Ostwald ripening") or to the interaction of the yttria particles with aluminium dissolved in the matrix. Unlike the latter process, only the former would increase the average dispersoid spacing and thereby degrade the strength of the alloy. There is indeed evidence suggesting that the dispersoids consist of mixed yttrium-aluminium oxides, whose composition can change during high temperature exposure /16/.

Because of differential thermal contraction on cooling from processing temperatures, the dispersoids give rise to significant misfit strains in the matrix surrounding them. Under two-beam conditions, characteristic strain contrasts can be made visible in the TEM at room temperature (Fig.1), which suggest that the dispersoid puts the matrix locally in compression /17/. This effect may influence the room temperature strength of the alloy, but disappears at elevated temperatures.

2.2. Grain Structure and Texture

In order to reduce the detrimental effect of grain boundaries in high temperature service, their density perpendicular to the principal loading direction must be minimized. This is achieved by a high temperature recrystallization heat treatment (see 3.3.). The resulting grain structure is shown in Fig.2: the grains, typically several centimeters in length, are highly elongated, with grain aspect ratios of 10 and more. The grain boundaries are highly serrated, enabling neighbouring grains to interlock with each other.

Another effect of recrystallization is the development of a strong texture. In MA 6000, a <110> texture is invariably produced /18,19/, which is not desirable from the point of view of thermal fatigue resistance and intermediate temperature creep strength. For MA 956 /20, 21/ higher-index textures have been reported which result from isothermal annealing.

2.3. Other Microstructural Details

Apart from oxide dispersoids and gamma' precipitates, MA 6000 also contains occasional coarser particles, as illustrated in Fig.3 /11/. These have been identified to consist of titanium carbonitrides (transparent and facetted) and of aluminium oxide (more opaque and round). Also some features which have to be classified as processing defects have been detected frequently /22/, in particular insufficiently recrystallized regions with a chemical composition identical to that of the base material. Other common processing defects are solute-rich particles, e.g. Cr-rich inclusions.

The occasional coarser particles as well as the processing defects are found to be aligned in the form of stringers parallel to the extrusion direction (Fig.4 /19/). They are expected to influence the grain

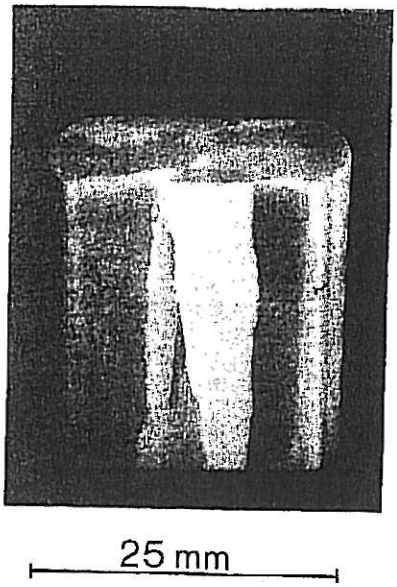

Fig. 2: Optical micrograph showing large elongated grains of MA 6000

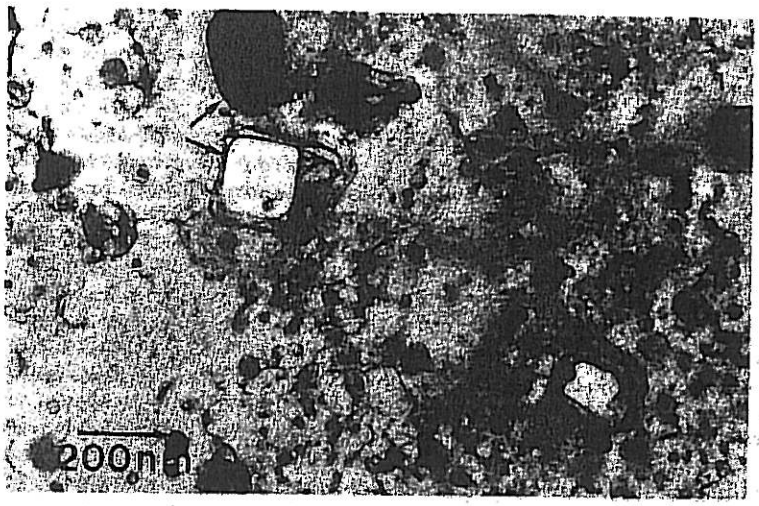

Fig. 3: Titanium carbonitride (transparent and facetted) and aluminium oxide particles (opaque) in MA 6000 /11/

coarsening behavior during zone annealing (see 3.3.), creep strength, fatigue strength, and transverse ductility.

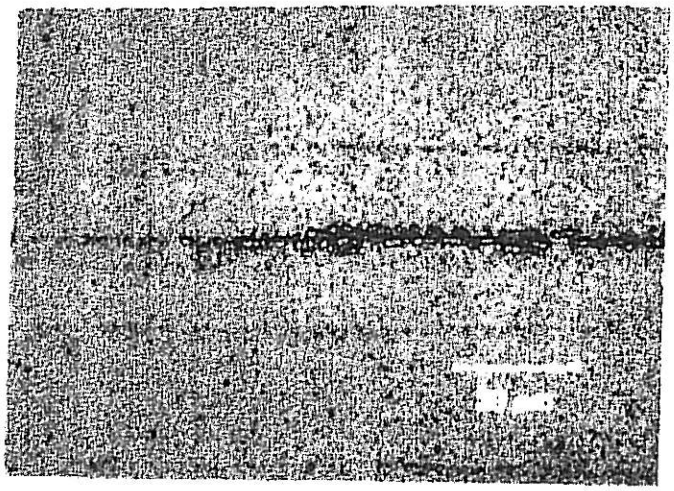

Fig. 4: Stringer-like processing defect in MA 6000 /19/

3. PROCESSING

3.1. Mechanical Alloying

Both MA 6000 and MA 956 are produced by mechanical alloying, which is a dry, high energy ball milling process /23,24/. The raw materials are added in form of elemental or prealloyed powders which are repeatedly cold welded and fractured during mechanical alloying. The feature distinguishing mechanical alloying from conventional ball milling is the much higher energy input. While conventional ball milling reduces the size of the powder particles, the high energy environment in mechanical alloying promotes welding and the powders remain relatively coarse.

The mechanical alloying process as part of the fabrication of ODS materials, Fig.5, serves three objectives at the same time:

(1) It creates a uniformly alloyed powder from a blend of elemental and prealloyed starting powders. Detailed investigation has shown that true solid solutions with elemental components interdispersed on an atomic scale can be formed /25/.
(2) Mechanical alloying serves to introduce a homogeneous oxide dispersion.
(3) Mechanical alloying produces strong work hardening in the powder particles. The result is a very high energy content in the powder, i.e. a very high dislocation density and small grain (subgrain) size, see Fig. 6.

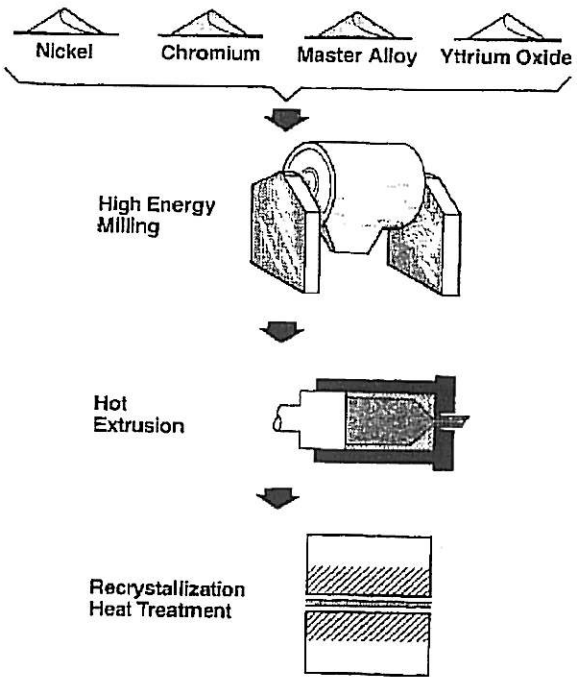

Fig. 5: Process for manufacture of an oxide dispersion strengthened superalloy

On a laboratory scale mechanical alloying has been performed successfully in various types of ball mills. Benjamin and his co-workers at Inco, to whom much of the credit for developing the process must go, worked wich Szegvari attritor grinding mills where the ball charge is activated by impellers radiating from a vertical central shaft. The capacity of the attritors used ranges from 4 to 400 liters and the central shaft is rotated at frequencies of up to 4 Hz. Work at C.E.N. in Belgium has shown that vibratory ball mills are also suitable for the manufacture of ODS alloys /26/. A major step forward was the up-scaling of the mechanical alloying process at Inco by successful application of large horizontal ball mills in 1983 /27/. The rotating element is a 2.6 meter long, 2 meter diameter steel drum loaded with 1 ton of powder and more than 10 tons of steel balls. Highly energetic milling conditions are achieved by (1) operating the mill just below the critical speed that would pin the balls to the internal walls of the mill, (2) reducing the weight of the powder charge relative to the ball charge, and (3) selecting a large mill diameter. It also seems likely that milling under somewhat less energetic conditions can be compensated for by lon-

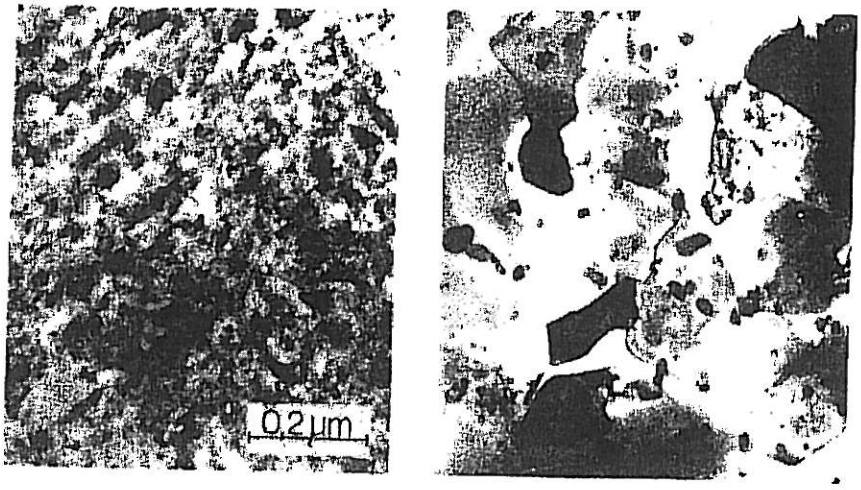

Fig. 6: Transmission electron micrographs showing the small grain size and high dislocation density in mechanically alloyed powder (left) and the somewhat larger grain size in extruded bar of MA 6000 (right)

ger milling times. This is suggested by results of Coheur, shown in Fig. 7.13 in Ref./9/.

Alloys with a high content of alloying elements, such as MA 6000, have not yet been made successfully in a large scale process, e.g. by milling in large horizontal ball mills. However, another important processing improvement has been made for MA 6000 lately: The original ten component system of raw material powder, Table 1 in Ref./5/, has been replaced by a three component system /28/. This change could be realised by utilization of an argon atomized omnibus master alloy. The omnibus master alloy helps to lower the stringer content in the material because of the greater homogeneity at the start of mechanical alloying and retarded reaction of alloying elements. A lower content of stringers is beneficial to transverse ductility and fatigue strength since stringers may act as crack initiation sites. The stringers are probably also the cause for inferior grain structures, and therefore are detrimental to rupture strength.

It is interesting to note that Smith and Grant /29/ were successful in fabricating an IN 100 type ODS alloy from fully alloyed powder, an approach which might improve properties even further.

The alloy MA 956 is produced in an argon atmosphere /12/ in the process presently used at Inco. During mechanical alloying, argon is entrapped which leads to porosity formation during high temperature exposure and a subsequent deterioration of properties (see 4.5). Studies by Coheur at C.E.N. in the framework of COST /30/ have shown that ferritic ODS alloys can be produced without use of argon. This indicates a potential way of further improving the properties of this alloy.

Although there are still some problems to be solved, mechanical alloying remains at present the most promising production route for alloys like MA 956 and MA 6000. It is interesting to note, however, that alternative processes are also under development. One example is the spray-dispersion method developed by Japanese researchers /31/. Oxide particles are sprayed under high pressure into a molten metal stream. The dispersoid spacing is not yet comparable to that achieved by mechanical alloying, but considerable improvements could be obtained by adding certain alloying elements and interesting mechanical properties have been demonstrated, Fig.7 /31/.

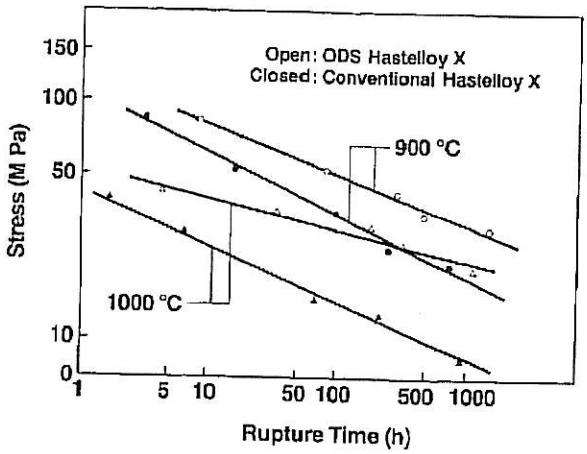

Fig. 7: Creep rupture strength improvement for ODS Hastelloy X prepared by spray-dispersion /31/

3.2. Powder Consolidation

The method employed to consolidate MA 6000 and MA 956 is hot extrusion. The structural changes during extrusion are manifold and rather complex:

(1) 100% density is achieved by deformation and welding of powder particles.

(2) Larger oxide and carbonitride particles and brittle underprocessed particles are fragmented and transformed into stringer-like arrangements.

(3) The energy content is adjusted in order to develop optimum grain structures in the subsequent recrystallisation heat treatment.

(4) Chemical and structural homogeneity is improved. The extent of homogeneity achieved is demonstrated by the fact that in MA 6000 a gamma'-precipitation structure is observed after extrusion which is probably formed during extrusion and subsequent cooling.

The adjustment of the energy content for subsequent recrystallization requires a careful optimization of extrusion conditions. Such an optimization - on a trial and error basis - has been described in detail for MA 6000 /32/. The structural changes associated with the energy adjustment are apparent from Fig.6: Considerable grain growth and reduction of dislocation density take place. It seems that a certain grain size and dislocation density is necessary in order to obtain the optimum recrystallization response. This situation is described schematically in Fig.8.

A rough estimate of the energy content in the as-extruded condition for MA 6000 shows /33/ that grain boundaries store about three orders of magnitude more energy than dislocations. This means that the grain size is the main structural feature to be considered in the energy adjustment process. It should be noted that no distinction is made in this context between grain size and subgrain size because it is virtually impossible to separate the two experimentally.

The structural changes during extrusion might be due to dynamic recovery or dynamic recrystallization. Static recrystallization during cooling from the extrusion temperature can be ruled out based on the dislocation content of the material /33/. The changes of grain size (subgrain size) during dynamic recrystallization and dynamic recovery have been studied in detail for a number of model materials (Fig. 13 and 36 in Ref./34/). The grain size (subgrain size) depends on strain rate and temperature during deformation. Considerable strain is necessary to establish a new grain size.

Attempts were made to use HIP'ing rather than hot extrusion to consolidate MA 6000 /35/. Annealing treatments were used in an effort to adjust the grain size in a similar way as during hot deformation - with no success. It seems that the structural and chemical homogeneity of the material is not sufficient for energy adjustment by annealing: As shown schematically in Fig.8b, the particular annealing treatment which is sufficient to adjust the grain size in some parts of the material might lead to excessive growth in other parts. Chemical heterogeneity could play a similar role as initial spread of grain size distribution, e.g. variation in gamma'-size and volume fraction might prevent successful recrystallization.

The structural changes during extrusion of MA 956 seem to be similar to MA 6000 /12/. One difference is that MA 956 exhibits a texture in the as-extruded condition which MA 6000 does not /12,36/. The reason for the different behavior may be the extremely fine grain size in MA 6000 which leads to substantial grain-boundary sliding and grain rotation during deformation, hereby preventing texture formation.

3.3. Recrystallization Heat Treatment

Stress rupture strength of the as-extruded fine grain material is very low. In order to develop useful strength, the material must be recrystallized to large elongated grains.

Recrystallization of MA 6000 has been studied in much detail /33/. It can be shown that the large grains form by a mechanism similar to secondary rather than primary recrystallization. In a strict sense,

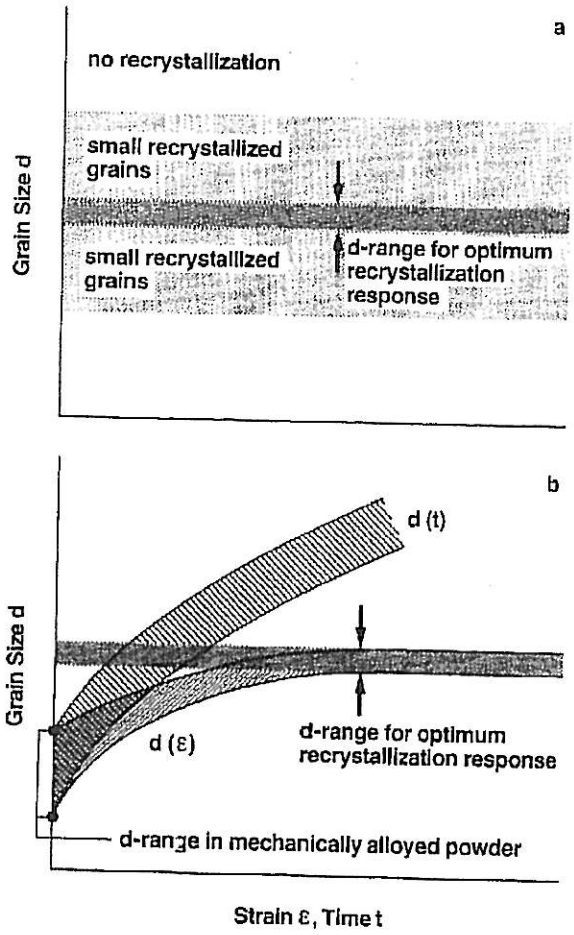

Fig. 8: Schematic representation of grain size adjustment (energy content adjustment) during processing for subsequent recrystallization

a): The recrystallized grain size depends on the primary grain size d which is plotted on the ordinate. There is only one particular primary grain size which gives an optimum grain size in the subsequent recrystallization. Both smaller and larger primary grain sizes d result in inferior recrystallized structures.

b): Extrusion under the right condition results in controlled coarsening of the primary grain structure (d (ε)). Annealing is less suitable for grain size adjustment (d (t)) because it does not narrow the grain size distribution

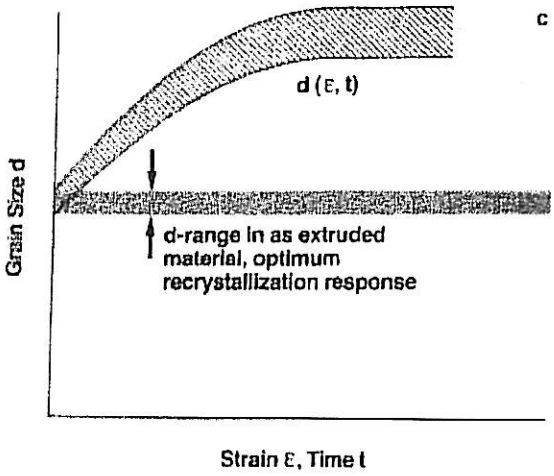

c): Deformation or annealing of the extruded material can lead to additional undesirable growth of primary grains which prevents subsequent recrystallization

primary recrystallization has not yet occurred, but the driving forces and retarding forces are typical for secondary recrystallization: Due to the extremely small grain size (0.2 µm), most of the driving force is stored in the grain boundaries. Recrystallization is triggered by gamma'-dissolution /37/ which occurs at roughly 1165°C. The largest grains are formed at recrystallization temperatures just above the critical temperature.

Once the driving forces become smaller than the retarding forces, secondary recrystallization is suppressed /33/, Fig.8a. It is less clear why the recrystallized grain size goes through a maximum with increasing driving force, i.e. why it increases first and then starts to decrease again (Fig.8a,9 /38/). One might presume that this is caused by the different dependence of growth rate and unpinning rate on driving force. A detailed analysis shows that minor differences in the increase of growth rate and unpinning rate with driving force are sufficient to explain large variations of the recrystallized grain size /39/.

In order to increase grain size and grain elongation as much as possible, zone annealing (gradient annealing) is used for MA 6000 rather than isothermal annealing. The temperature gradient suppresses nucleation of new grains and encourages growth competition among existing grains. Allen /40/ was first to demonstrate the beneficial effect of zone annealing on structure and properties of ODS alloys.

There are two important parameters in zone annealing: the temperature gradient and the rate of specimen movement through the gradient /40,41/. While the gradient obviously must be as high as possible, some intermediate travel rate in the order of mm/min is found to be optimum.

Too low a travel rate leads to growth of primary grains and undesirable loss of driving force. A travel rate too high seems to be disadvantageous because the velocity of grain boundary movement is rather small. As such, too high a travel rate makes it difficult for the large grains to follow the hot zone /39/.

MA 956 develops sufficently large and elongated grains during isothermal annealing, therefore zone annealing is not required /12,42/. It has been speculated /42/ that the difference is due to the larger window available for heat treatment, i.e. the higher melting temperature and lower critical grain coarsening temperature.

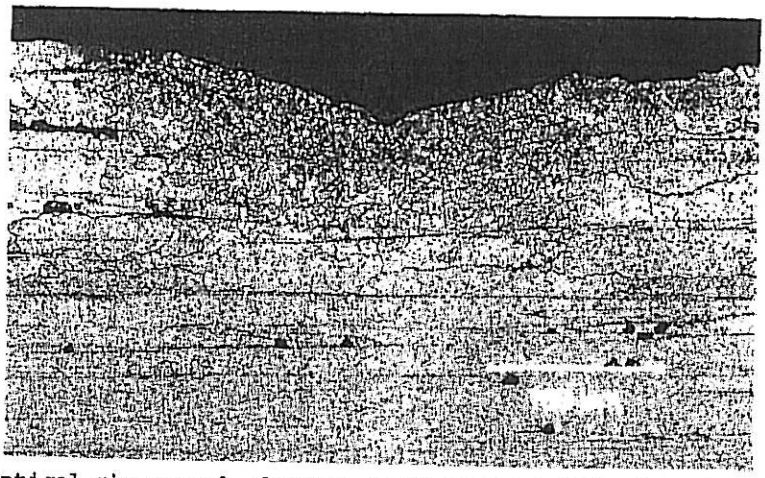

Fig. 9: Optical micrograph showing small recrystallized grains in MA 6000 close to a hardness indentation /38/. The hardness indentation has been applied in the as extruded state and the material went through a recrystallization heat treatment afterwards. The room temperature deformation changed the energy content and affected the recrystallized grain size

3.4. Forging

The high cost of ODS components have discouraged more wide spread use. Near-net shape and net shape forging are potential cost saving processes because they provide better material utilization. Material utilization in turbine blade manufacturing by machining from rectangular extrusion can be as low as 8% /43/.

Complex alloys, like MA 6000, cannot be forged in the recrystallized state because of their low ductility. Hot working in the fine-grain as-extruded condition is possible; the alloy even behaves superplastically in a certain temperature and strain rate regime /44,45/. Care has to be taken, however, that the driving force for subsequent recrystallization is not lost by excessive grain growth during hot working. This problem is represented schematically in Fig.8c. The change in primary grain size and recrystallization response as a function of deformation rate and temperature can be described conveniently by use of the diffu-

sion-compensated strain rate, Fig.10 /33/. Hot working conditions which avoid undesirable growth of primary grains turn out to yield low ductility and high die loads. Careful control of the forging conditions is therefore necessary. Although the feasibility of forging has been demonstrated, further development work will be necessary to make it a viable production process.

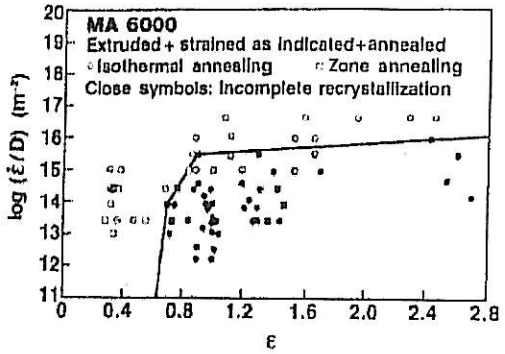

Fig. 10: Influence of deformation conditions on response to subsequent recrystallization. Open symbols indicate combinations of diffusion compensated strain rates and strains which lead to material which can be recrystallized subsequently. Closed symbols indicate conditions which prevent subsequent recrystallization /33/

MA 956 is much more amenable to forging because of its lower strength and higher ductility. A large variety of shapes have already been fabricated by a number of forming techniques /46/. An interesting phenomenon is the embrittlement of MA 956 during high temperature exposure due to formation of a highly adherent oxide scale which induces cracks in the base metal /47/. This can also lead to fabrication problems.

4.5. Joining

Problems in finding adequate joining methods have been another reason for reluctance to use ODS alloys. The most economical joining technique, fusion welding, results in rather low joint strength /48-50/. The reason is that the oxide dispersoids agglomerate into detrimental inclusions and that a cast grain structure with small dispersoid free grains is generated.

Brazing is a more suitable joining technique for ODS alloys since only a small volume of material is liquified and oxide agglomeration is less severe. Brazing is also commercially used for the fabrication of ODS turbine vanes /1/. A considerable amount of work on brazing has been carried out within the COST 501 program. It could be shown that joint strength slightly lower than for conventional superalloys can be achieved in MA 6000 /51,52/. This means that joint efficiency in MA 6000 is almost equal to that in conventional alloys in the transverse

direction (where strength is similar), and joint efficiency is inferior to conventional alloys in the longitudinal direction (where strength of MA 6000 is higher). Care has to be taken in selecting brazing alloy compositions to avoid Kirkendall porosity. Basically, if the matrix alloy is leaner than the brazing alloy, vacancies will diffuse into the brazing alloy where void formation is less likely than in the ODS alloy. Hot corrosion and thermal fatigue resistance of brazings are important considerations which will need more attention in the future /52/. Another interesting result from the COST 501 work was that PVD is not suitable for application of boron-containing brazing alloys, probably because boron is not precipitated as it is in tapes or powders and diffuses rapidly out of the coating /53/.

If base metal properties have to be achieved in the joint, diffusion welding techniques must be used for ODS alloys. Diffusion welding is a solid-state joining process by which two clean surfaces are joined at elevated temperature under an applied interfacial pressure. The problems of liquid phase joining techniques, like oxide agglomeration, fine grain and dispersoid free joint zone, can be avoided.

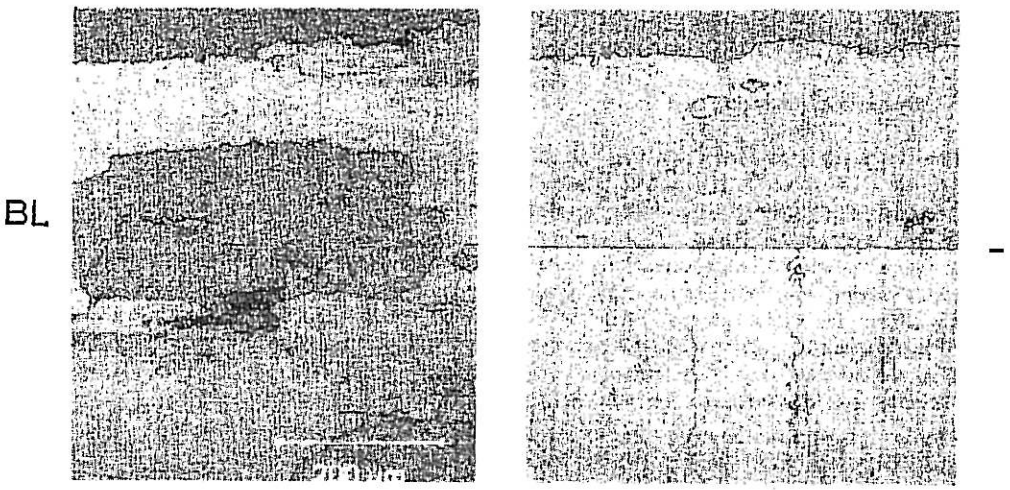

Fig. 11: Diffusion welding of MA 6000. The optical micrographs show the joint structure for material welded in the unrecrystallized condition which was subsequently recrystallized (left) and for material which was welded in the recrystallized condition (right) /54/

Diffusion welding of MA 6000 can be done successfully in the recrystallized or unrecrystallized condition as demonstrated by Fig.11 /54/. When diffusion welding is carried out in the unrecrystallized condition, welding must be followed by the usual recrystallization heat treatment. It is then often found that some smaller grains are present in the weld interface /55,56/. This is due to unsuitable machining pro-

cedures or welding conditions which change the energy content in the material as described above. The main problem in diffusion welding of recrystallized material is the limited compressive ductility of MA 6000 in the recrystallized condition /55,56/. It is obvious from Fig.11 that the material welded in the recrystallized condition exhibits a straight grain boundary in the weld interface which might result in properties slightly inferior to the base metal.

Joining of MA 956 follows similar principles as described above for MA 6000 /49,56/. In general, joining conditions are somewhat less critical than for MA 6000.

3.6. Machining

Machinability of ODS alloys is not much different from that of other well-established superalloys /57,58/. MA 6000 is similar to Udimet 700 and better than IN 713 and IN 738. ODS alloys are also amenable to electrical-discharge and electrochemical machining (EDM and ECM). It has been noted that MA 6000 gives extremely good surfaces in ECM /59/.

4. PROPERTIES OF ODS SUPERALLOYS

4.1. Physical Properties

Of the two alloys considered in this paper, MA 6000 is somewhat heavier (density 8.1 g/cm^3) than MA 956 (7.2 g/cm^3) and has a lower solidus temperature (1296°C vs. 1482°C for MA 956). The elastic moduli of MA 6000 are shown in Fig. 12 /36,60/. It can be seen that in the as-extruded, unrecrystallized condition neither Young's modulus nor the shear modulus show any directional dependence, which attests to the absence of texture in this state. After recrystallization, which is accompanied by the formation of a <110> texture, Young's modulus depends strongly on the orientation. For comparison, Young's modulus of MA 956 in the longitudinal direction is also included in the figure.

4.2. Yield Strength and Tensile Ductility

The yield strength of ODS superalloys is the result of the superposition of several strengthening mechanism: (i) solid solution strengthening, (ii) precipitation strengthening, and (iii) dispersion strengthening (see also Ref./9/). The theoretical understanding of the two latter mechanism, which are most important in ODS alloys, has been reviewed by Brown and Ham /61/. Dispersion strengthening is of particular interest here; it arises because the dispersoids force lattice dislocations to bow out between them. This so-called "Orowan mechanism" /62/ requires a critical stress which in its simplest form is given by:

$$\sigma_{or} = 0{,}84\ \mathrm{GbM/l} \qquad (1)$$

where G is the shear modulus of the matrix, b the Burgers vector of a lattice dislocation, M the Taylor factor, and l the mean planar dispersoid spacing. The increase in strength according to eq. (1) may reach several hundred MPa in MA 6000 and MA 956 with a mean dispersoid spacing of about 100 nm.

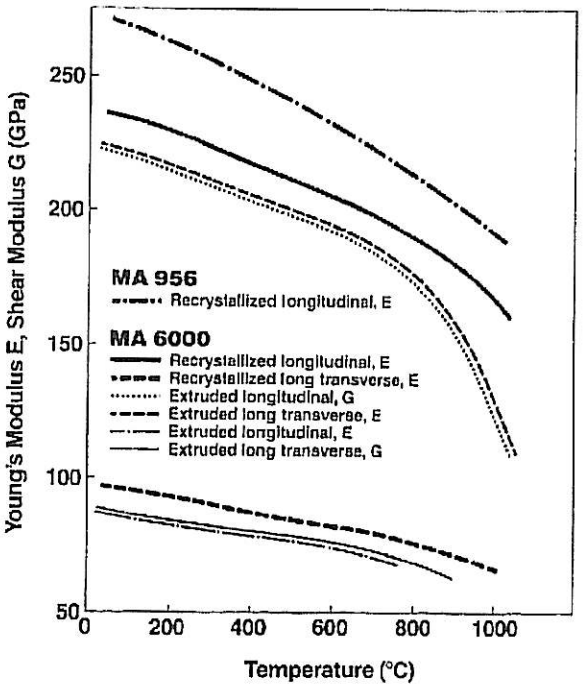

Fig. 12: Elastic moduli of MA 6000 /36/ and MA 956 /60/ as a function of temperature

The influence of texture on the room-temperature strength enters through the numerical value of M. It has been argued /9/ that MA 6000 is "texture weakened" rather than "texture strengthened": in the <110> texture, glide planes are oriented favorably with regard to a stress applied in the direction of grain elongation, giving a low value of M (M = 2.45).

For MA 6000 the contributions of dispersion strengthening and precipitation hardening to the room-temperature yield strength have been estimated /63/. When Orowan bowing between the oxide dispersoids in the matrix and pairwise cutting of the gamma' precipitates, weighted by their volume fraction, are considered to superimpose linearly, then close agreement with the measured yield stress is obtained.

Yield and tensile strengths of MA 6000 and of MA 956 as a function of temperature are plotted in Fig.13 /60/. The strong precipitation hardening in the case of MA 6000 gives rise to a much higher strength and stronger temperature dependence as compared to MA 956: at very high

temperatures the strength levels become more similar because dispersion hardening is left as the only potent strengthening mechanism in both alloys.

The ductilities of ODS alloys in the longitudinal direction amount to reasonable values (5-10% /60/). When tested in the long-transverse direction, however, these alloys exhibit extremely low ductility and shear strength /64,65/. This weakness can be attributed to the presence of the stringers of inclusions (see Fig.4), which crack or debond from the matrix. For MA 6000 batches with varying inclusion content, a correlation has been established between room-temperature ductility and a geometrical parameter describing the projected length of the stringers /64/. It shows clearly that transverse ductility can be improved substantially by reducing the inclusion content. As such, great importance must be attached to the development of cleaner ODS alloys, as described in section 3.1., in order to alleviate the transverse ductility problem.

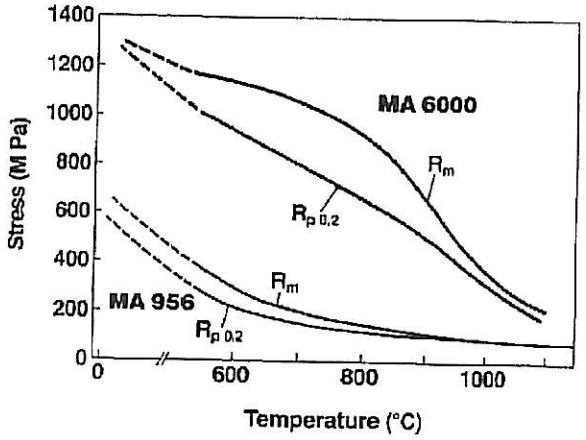

Fig. 13: Yield strength (0.2% offset) and tensile strength of MA 6000 and MA 956 as a function of temperature /60/

4.3. Creep Strength

Coarse-grained materials deform at high temperatures by "dislocation creep" (also called "power-law creep"). The strain rate $\dot{\varepsilon}$ is then proportional to some power n of the applied stress σ, and the constitutive equation can be written, for example, as:

$$\dot{\varepsilon} = A\, D\, (\sigma/E)^n \qquad (3)$$

where D is the lattice diffusivity, E Young's modulus and A a material constant. This semi-empirical equation holds for many high-temperature materials and can in principle be applied to ODS alloys as well.

The minimum creep rates of MA 6000 and MA 956 as a function of the applied stress are plotted in Fig.14. Following common practice, the rates have been normalized by the lattice diffusivity and the stress has been normalized by E. For comparison, the data for fine-grained (unrecrystallized) material and for Ni-20 Cr are also included.

The effect of the dispersoids in the coarse-grained materials is to lower the creep rates and to increase the stress exponent n to 20-40, which is far beyond the values typical of conventional superalloys. Such a high stress sensitivity is best described by invoking a "threshold stress" below which the creep rates are considered to be negligible /69-72/. The data then follow a modified constitutive equation:

$$\dot{\varepsilon} = A\,D\left(\frac{\sigma-\sigma_{th}}{E}\right)^{n'} \qquad (4)$$

where σ_{th} is the threshold stress and n' a new stress exponent. Eq. (4) has been verified for MA 6000 using a stress exponent n' = 3.5 and fitting the numerical value of σ_{th} /66/.

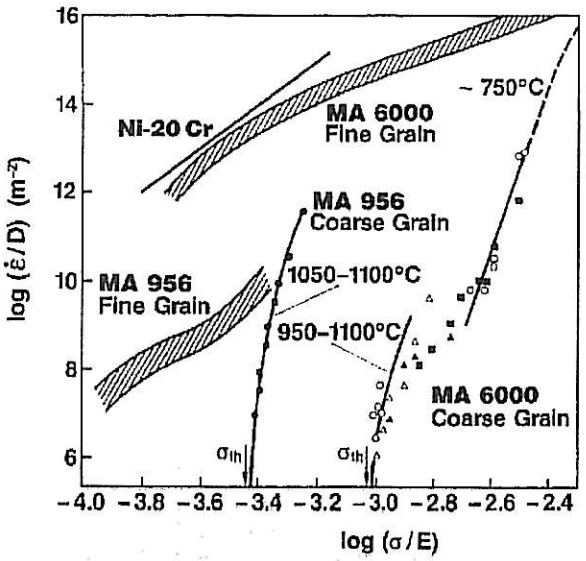

Fig. 14: Diffusion-compensated creep rates as a function of modulus-compensated applied stress for MA 6000 and MA 956. The data was taken from Ref./13,14,60,66,67/, E values from Fig.12, $D = 1.9 \cdot 10^{-4} \exp(-284.000/RT)$ m^2/sec for MA 6000 and $D = 2 \cdot 10^{-4} \exp(-251.000/RT)$ m^2/sec for MA 956 /60/. Strength values of fine-grained materials and of Ni-20Cr are shown for comparison

The threshold stress is not strictly a material constant but drops in MA 6000 with increasing temperature as seen clearly in Fig.14. The

reason is that gamma' precipitates, whose volume fraction diminishes with increasing temperature, contribute to the threshold stress at 760°C but less so at the higher temperatures. Ultimately, at very high temperatures, the expected threshold amounts to about $9 \cdot 10^{-4}$ E (100 MPa) in MA 6000 and to $4 \cdot 10^{-4}$ E (60 MPa) in MA 956.

It is important to note that in the fine-grained condition neither alloy exhibits a threshold stress of similar magnitude. This fact, which is due to the occurrence of grain boundary sliding and interface-controlled diffusion creep (see e.g. /13,73/), is exploited in forming operations (chapter 3.4.). We note in passing that the general appearance of Fig.14 is not unique to the two alloys considered, but is typical of dispersion-strengthened systems /69,74/.

For the stress rupture behavior of MA 6000 a much broader data base has been established, as shown in Fig.15 /75/. The high stress sensitivity is reflected here in the shallow slope of the curves. Unlike conventional alloys, the curves are concave upward and seem to level off at long lives and high temperatures. This observation, which is compatible with the strain rate data in Fig.14, has lead to a somewhat arbitrary but useful delineation of Fig.15 in two regions /75/: in region I (high stress, short lives) the stress sensitivity is much lower than in region II (low stress, long lives). This is of great importance for the extrapolation to long lives which will be over-conservative when based on data in region I.

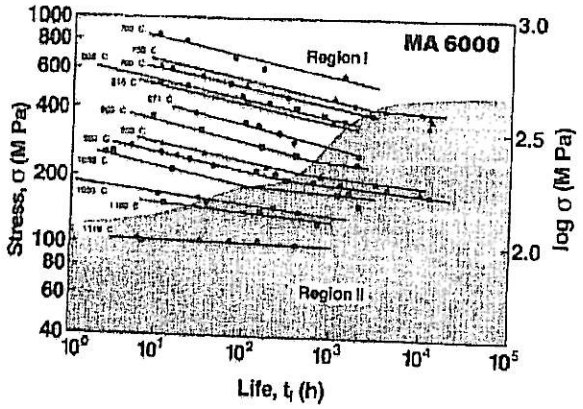

Fig. 15: Stress rupture behavior of MA 6000 /75/

From a pragmatic point of view, the concept of a threshold stress is useful because it explains the high strength and high stress sensitivity which would be difficult to rationalize otherwise. Scientifically, a more thorough understanding of the mechanisms leading to such a threshold and in particular a quantitative correlation between threshold stresses and microstructural parameters is desirable. The origin of the ultimate threshold stress at very high temperatures must lie in the interaction of lattice dislocations with the oxide dispersoids. The mechanism for this process is complicated by the fact that high tempe-

ratures enable dislocations to circumvent hard particles by climbing around them. For this process a number of models have been developed /76,77,78/ which suggest that the threshold stress is some fraction of the Orowan stress.

A recent TEM study, performed in COST 501, of the dislocation mechanism in MA 6000 /79/ has revealed an attractive interaction between dispersoids and dislocations at high temperatures (Fig.16 /79/), similarly as in an earlier study on a gamma'-free ODS alloy /80/. Such an attraction has in fact been expected on theoretical grounds /13,81/, because a dislocation can relax its strain field in the vicinity of a slipping particle-matrix interface. Theoretically it has been shown /82/ that only a small attractive interaction is required in order to bring a new strengthening mechanism into the foreground: the detachment of dislocations from the departure side of dispersoids over which the dislocations have climbed. The threshold stress for this process depends on a parameter k describing the relaxation of the dislocation and is proportional to the Orowan stress:

$$\sigma = \sigma_{or} \sqrt{1-k^2} \qquad (5)$$

This approach may eventually lead to a better understanding of threshold stresses and allow a more rational exploitation of dispersion strengthening in high temperatures alloys. More details are to be found elsewhere in this volume /83/.

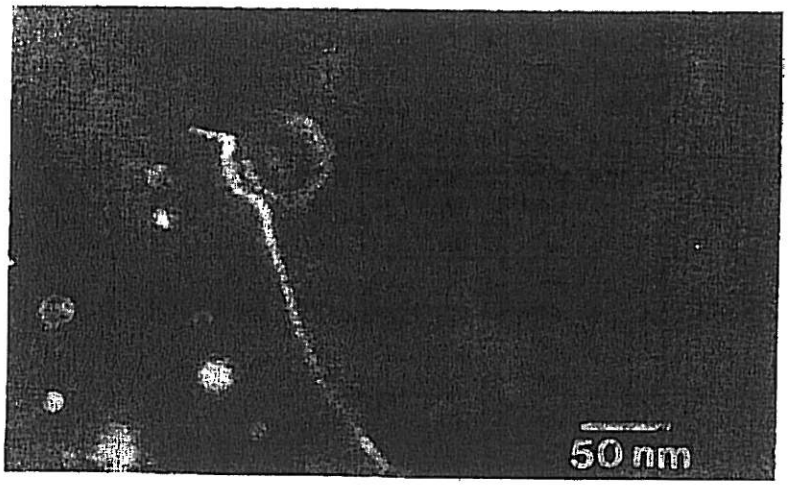

Fig. 16: TEM dark field micrograph showing attractive interaction between a lattice dislocation and a dispersoid during creep of MA 6000 /79/

So far we have been concerned with the longitudinal creep behavior of well recrystallized material with a grain aspect ratio (GAR) of more than 10. Under these conditions the grain boundaries do not influence

the deformation behavior, and creep fracture is transgranular. It was realized early in the development of ODS alloys that a sufficiently elongated grain shape is indispensable for achieving optimum properties. At low GAR values, rupture times may be reduced by more than two orders of magnitude, as is shown for MA 6000 in Fig.17 /84/. The reason is that in such high-strength grains, loaded at temperatures relatively close to the melting point, a transverse grain boundary constitutes an extremely weak microstructural element: Damage in the form of creep cavities develops on these boundaries (Fig.18 /22/) and leads to premature intergranular failure. The effect of grain shape has been explained in terms of damage accommodation by grain boundary sliding /84/. A similar damage mechanism may be responsible for premature failure of MA 6000 under creep in a direction perpendicular to the grain elongation. This might explain the very low stress rupture strength of MA 6000 in this direction /19/.

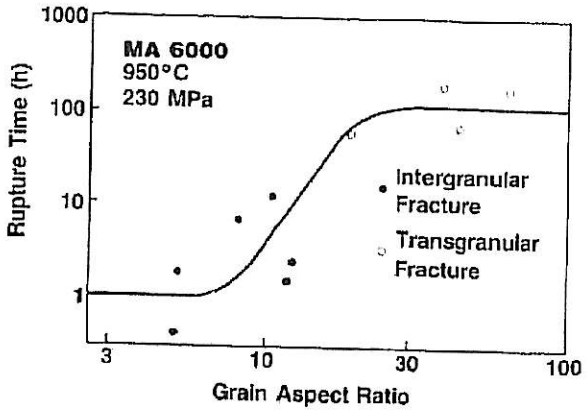

Fig. 17: Dependence of creep rupture time on grain shape /84/

In MA 6000 with a GAR of more than 10, creep exposure is accompanied by the development of localized damage at processing defects and on transverse grain boundaries, but subsequent fracture is transgranular and not affected by these damage processes. Evidence of gamma' coarsening and rafting at 950°C has been reported /14/. The average dispersoid diameter increases after 10.000 h at this temperature by a factor of almost 2, with apparently no serious loss in the load-bearing capability of the alloy indicating dispersoid-matrix interaction rather than dispersoid coarsening /14/ (see discussion in chapter 2.1. on dispersoid coarsening).

4.4. Fatigue Strength

The fatigue strength of properly processed ODS alloys can generally be expected to match or even surpass that of their conventional cast counterparts because of (i) the possibility of slip dispersal at the dispersoids, (ii) the absence of casting pores and resulting retardation of crack initiation, and (iii) texture effects.

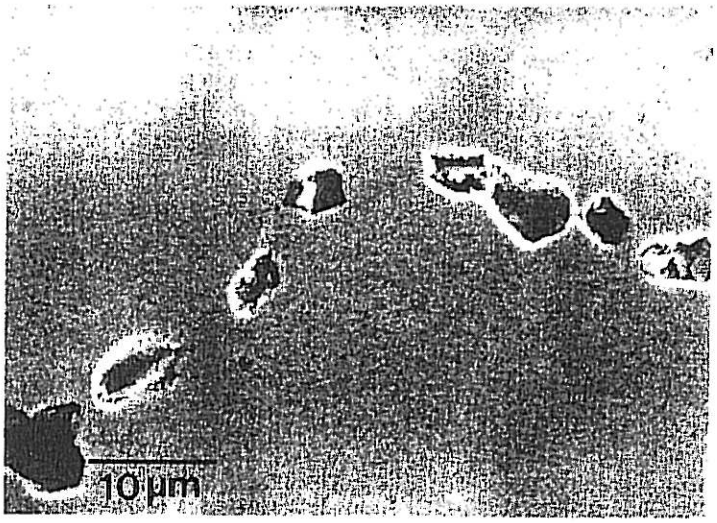

Fig. 18: Creep cavities on a transverse grain boundary in MA 6000. Note particle-free zones at the boundary suggesting diffusional cavity growth /22/

An early study of MA 6000 indeed confirmed this view by encountering an unusually high endurance ratio /85/. Recently, HCF of MA 6000 has been investigated in more detail /86/. HCF cracks were observed to develop from stringers of inclusions. It was also found (Fig.19 /86/) that longitudinal loading at 850°C results in HCF strength which is markedly higher than that of the conventional cast alloy IN 738 LC. This superiority was attributed mainly to a reduced size of potential crack nucleation sites and a higher threshold stress intensity range, as a result of a higher Young's modulus. In the transverse direction, the strength is reduced in proportion with the larger crack nucleation sites (stringers!) and the lower Young's modulus in this direction, but falls still within the scatterband for IN 738 LC. Crack growth rates were measured to be lower in the transverse direction on account of the occurrence of extensive crack branching at grain boundaries /86/.

High temperature low-cycle fatigue of MA 6000 has been studied extensively within the framework of COST 501 (see also /87/). The measured cyclic lives at 850°C are compared to those of IN 738 LC in Fig.20 /87/. It is apparent that the fatigue properties are almost identical when expressed in terms of the t o t a l strain amplitude, and somewhat superior when compared at similar p l a s t i c strain ranges. At about 1000°C a transition from transgranular to mixed trans/intergranular failure occurs, which is ascribed to the onset of environmental attack. Contrary to other high temperature materials, crack initiation takes up a significant portion of fatigue life.

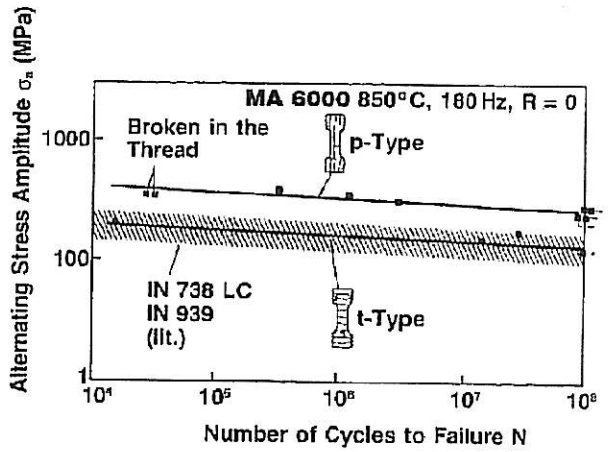

Fig. 19: HCF strength of MA 6000 in two orientations as compared with the conventional cast alloy IN 738 /86/

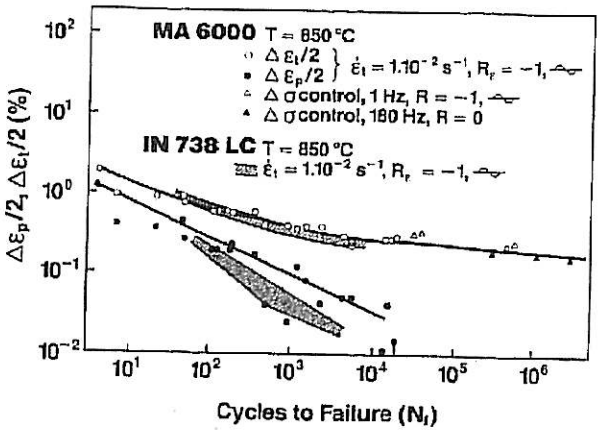

Fig. 20: LCF strength of MA 6000 as compared to the conventional cast alloy IN 738 /87/

4.5. Thermal Fatigue Resistance

Because of its high modulus, MA 6000 is expected to be "texture weakened" with regard to thermal fatigue. Nevertheless results obtained in COST 501 indicate that resistance to thermal fatigue is markedly better than that of the conventional cast alloy IN 100, though inferior to the

single-crystal alloy CMSX-2 /51/. MA 956, however, showed much poorer performance, which is attributed to the presence of pores developed during exposure to 1200°C and above /88/. These pores, which are filled with argon incorporated during mechanical alloying, induce tensile stresses in the surrounding matrix during cooling and are believed to thereby facilitate cracking. These findings are in general agreement with a study on several ODS alloys which concluded that, with the exception of MA 956, ODS superalloys are superior, in terms of thermal fatigue resistance, to conventionally cast superalloys and comparable with directionally solidified superalloys /89/.

4.6. Hot Corrosion Resistance

The lifetime of a stressed part in a gas turbine may be limited by its corrosion resistance rather than by its strength. Because ODS alloys are to be used at higher temperatures, where they offer the greatest improvement in strength, corrosion resistance may be of even greater concern than for conventional alloys.

In terms of sulfidation resistance, MA 6000 has been found to be slightly more or less resistant than IN 738, depending on testing conditions /59,90/. With respect to oxidation resistance MA 6000 is similar to IN 100 and better than IN 738 or IN 792 /59,91/. MA 956 exhibits excellent sulfidation and oxidation resistance /92/. This is not surprising because the alloy composition is basically a typical coating composition. It has been shown that the presence of Y_2O_3-particles

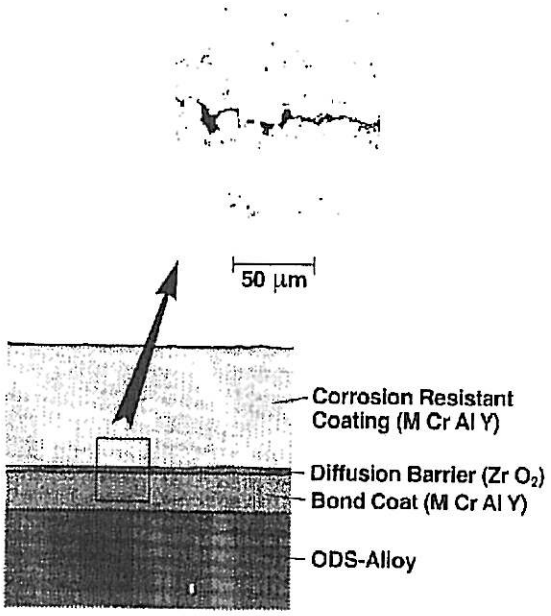

Fig. 21: Diffusion barrier coating on MA 6000 applied by low pressure plasma spraying /53/

improves hot corrosion resistance (for a review see /9/). The alloys MA 6000 and MA 956, however, behave as to be expected from their composition, i.e. the Y_2O_3-effect does not seem to be very large.

MA 6000 will require the use of some protective coating in most applications, particularly when the potentially increased temperatures and lifetimes are considered. Good results have been obtained with overlay coatings, i.e. MCrAlY type coatings produced using PVD or low pressure plasma spraying /93,94/. Interdiffusion between coating and base metal is a major problem at the very high temperatures at which MA 6000 is intended to be used. Aluminium and chromium will diffuse inwards and the resulting depletion of the coating might limit the life of the coating. Interdiffusion can also lead to porosity formation in ODS alloys, although with some coatings porosity was not observed /93/. In order to prevent interdiffusion, diffusion-barriers have been investigated /95,96/. Diffusion-barrier coatings have also been studied as part of the COST 501 action and very promising results have been obtained /97,98/. One of the systems under investigation exhibits a thin layer of stabilized ZrO_2, Fig.21. Because of the rather thin layer very good thermal fatigue properties could be obtained. Alternative systems are presently being investigated which avoid the high oxygen diffusivity of ZrO_2.

5. CONCLUSIONS AND OUTLOOK

In terms of technology, MA 6000 and MA 956 have reached a state of considerable maturity. Important property improvements over conventional alloys have been demonstrated. This includes creep rupture strength, fatigue strength, and oxidation resistance. Up-scaling of alloy manufacturing has been carried out successfully. Some problem areas still exist, depending on the alloy and the application under consideration. Component fabrication techniques are of particular concern, but consicerable progress has been made. Certain forming and joining techniques are now available. Coating development for MA 6000 has shown some encouraging results. The reasons for low transverse ductility in MA 6000 have been identified and improvements through processing modifications have been obtained.

The scientific understanding of the relation between structure, processing, and properties of ODS superalloys has also improved. The effects of grain shape on rupture strength have been rationalized, and a new mechanism for dispersion strengthening at high temperatures has been identified. We are beginning to understand the relation between processing conditions and the existence of stringers of inclusions. The effect of the stringers on rupture strength, fatigue strength and transverse ductility has been clarified. "Energy building" for subsequent recrystallization during processing of ODS alloys is now quite well understood.

In spite of the considerable progress in recent years there is still room for further improvement of ODS alloys:

(1) Optimization of composition.
Alloys can be developed which are better adapted to the needs of the particular application.

(2) Optimization of structure.
Further improvements of properties can be expected by optimization of the structure. The ultimate goal is a <100>-oriented ODS single crystal component without stringers of underprocessed particles.

(3) Optimization of fabricability.
Forming of alloys like MA 6000 is rather difficult. Based on our improved understanding it should be possible to develop alloys which exhibit better forgeability, i.e. better ductility and lower flow stress in the fine grain condition.

6. REFERENCES

/ 1/ W.Crawford, in: J.S.Benjamin, R.C.Benn (eds), Frontiers of High Temperature Materials II, Conf. Proceedings, Inco Alloys International, London, 1983, p. 272

/ 2/ R.W.Fraser, S.G.Berkley, B.Hessler: Metal Powder Report Oct. (1985) 556

/ 3/ H.F.Merrick, L.R.Curwick, Y.G.Kim: NASA Contract Report 135 150, 1977

/ 4/ Y.G.Kim, H.F.Merrick: NASA Contract Report 159 493, 1979

/ 5/ R.C.Benn, L.R.Curwick, G.A.J.Hack: 1980 Powder Metallurgy Group Meeting, Conference Preprints, The Metals, Society, 1980, Paper 16

/ 6/ R.C.Benn, in: J.K.Tien et al.(eds): Superalloys 1980, ASM, Metals Park, Ohio, 1980, p. 541

/ 7/ S.K.Kang, R.C.Benn: Met. Trans. 16 A (1985) 1285

/ 8/ M.Yamazaki: Progress in Powder Metallurgy, Conf. Proceedings, San Francisco, 1985

/ 9/ R.F.Singer, G.H.Gessinger, in: G.H.Gessinger, Powder Metallurgy of Superalloys, Butterworth, London, 1984, p.213

/10/ J.S.Benjamin, R.C.Benn (eds): Frontiers of High Temperature Materials II, Conference Proceedings, Inco Alloys International, London, 1983

/11/ J.H.Schröder: Ph.D.Thesis, Universität Stuttgart, 1986

/12/ J.Nutting, H.S.Ubhi, T.A.Hughes in: J.S.Benjamin (ed), Frontiers of High Temperature Materials, Inco MAP, New York City, 1981, p.33

/13/ R.Petkovic-Luton, D.J.Srolovitz, M.J.Luton, in: Ref./10/ p.73

/14/ R.F.Singer, R.C.Benn and S.K.Kang, in: Ref./10/ p.336

/15/ J.K.Tien, in: Ref./10/ Discussion Section, p.119

/16/ M.Raghavan, J.W.Steeds, R.Pekovic-Luton: Met.Trans. 13A (1982) 953

/17/ J.H.Schröder, W.Mader, E.Arzt: to be published

/18/ T.E.Howson, D.A.Mervyn, J.K.Tien: Met.Trans. 11A (1980) 1609
/19/ C.P.Jongenburger, M.Y.Nazmy, R.F.Singer: COST 501, Project CH 6, Final Report 1986
/20/ J.D.Whittenberger, P.T.Bizon: Int.J.Fatigue (1981) 173
/21/ J.D.Whittenberger: Mat.Sci.Eng. 54 (1982) 81
/22/ H.Zeizinger: Ph.D.Thesis, Universität Stuttgart, 1986
/23/ J.S.Benjamin: Met. Trans. 1 (1970) 2943
/24/ P.S. Gilman, J.S.Benjamin: Ann.Rev.Mater.Sci. 13 (1983) 279
/25/ T.K.Wassel, L.Himmel: US Army Tank-Automotive Command Research and Development Center, Warren, Michigan, Technical Report No. 12571, 1981
/26/ L.Coheur: Paper presented at the Poster Session of the Conference "High Temperature Alloys for Gas Turbines", Liège, 1978
/27/ B.Williams: Metal Powder Report, October (1983) 577
/28/ G.A.J.Hack, G.M.Mc.Colvin, M.P.Williams, in: PM Aerospace Materials, Conf. Proceedings, Vol II, Metal Powder Report Conference, Bern 1984, paper 19
/29/ C.H.Smith, N.J.Grant: General Electric Coporate Research and Development, Report No. 84 CRD 143, 1984
/30/ L.Coheur: Unpublished result
/31/ M. Hasegaera, M. Osawa: Met. Trans. 16A (1985) 1043
/32/ J.P.Morse, J.S.Benjamin, in: New Trends in Materials Processing, ASM, Metals Park, Ohio, 1974, p. 165
/33/ R.F.Singer, G.H.Gessinger: Met. Trans. 13A (1982) 1463
/34/ H.J.Queen, J.J.Jonas: Treatise on Materials Science and Technology 6 (1975) 393
/35/ R.F.Singer, G.H.Gessinger: Powder Metallurgy Int. 15 (1983) 119
/36/ M.Y.Nazmy, R.F.Singer, E.Török, in: C.M.Brakman, P.Jongenburger (eds), 7th Int. Conf. on Textures of Materials, Netherlands, Society for Mat.Sci.,1984, p. 275
/37/ R.K.Hotzler, T.K.Glasgow, in: I.K.Tien et al. (eds.), Superalloys 1980, ASM, Metals Park, Ohio, 1980, p. 455
/38/ M.N.Nazmy, R.F.Singer: Unpublished result
/39/ C.P.Jongenburger, R.F.Singer: Unpublished result
/40/ R.E.Allen, in: Superalloys-Processing, MCIC-Report 72-10, Metals and Ceramics Information Center, Battelle, Columbus, Ohio, 1972, p. X-1
/41/ R.L.Cairns, L.R.Curwick, J.S.Benjamin: Met.Trans. 6A (1975) 179
/42/ G.A.J.Hack, in: Ref. /10/, p.3
/43/ J.A.Stahl, R.J.Perkons, G.Bailey: Contract Report AFML-TR-79-4163, 1979
/44/ R.F.Singer, G.H.Gessinger, in: N.Hansen et al. (eds), Deformation of Polycrystals: Mechanisms and Microstructures, Proceedings of the 2nd Riso International Symposium, 1981, p. 365
/45/ J.K.Gregory, J.C.Gibeling, W.D.Nix: Met. Trans. 16A (1985) 777
/46/ E.Grundy, W.H.Patton, C.J.Precious, D.Pinder, in: Ref./10/, p.100
/47/ T.Hughes, T.Hirst, in: Ref./10/, p.149
/48/ T.J.Kelly, in: J.S. Benjamin (eds.), Frontiers of High Temperatures Materials, Conference Proc., IncoMAP, New York City, 1981, p.111

/49/ T.J.Kelly, in: Ref./10/, p. 129
/50/ R.Thamburaj, R.F.Singer, G.H.Gessinger, in: G.H.Gessinger, Powder Metallurgy of Superalloys, Butterworth, London, 1984, p. 295
/51/ P.Adam, D.Froschhammer, H.Wilhelm: COST 501, Project D 48, Interim Report No.2, 1984
/52/ B.Jahnke, G.Dannhäuser: COST 501, Project D 39, Interim Report No. 2, 1984
/53/ I.A.Bucklow: COST 501, Project UK 5, Interim Report No. 3, 1985
/54/ H.Rydstad, R.F.Singer, in: Conference Proceedings PM'86 in Europe, Düsseldorf 1986, to be published
/55/ T.J.Moore, T.K.Glasgow: Welding Research Supplement, August (1985) 219
/56/ G.Haufler, H.G.Mayer: COST 501, Project D 42, Interim Report No. 2, 1984
/57/ J.A.Vaccari: American Machinist, December (1984) 64
/58/ R.C.Benn, in: Ref./10/, p. 37
/59/ G.S.Hoppin, F.A.Schweizer, in: J.S.Benjamin (ed) Frontiers of High Temperature Materials, Conf. Proc., IncoMAP, New York 1981, p. 75
/60/ IncoMAP data sheet
/61/ L.M.Brown, R.K.Ham, in: A.Kelly, R.B.Nicholson (eds), Strengthening Methods in Crystals, Elsevier, Amsterdam, 1971, p.9
/62/ E.Orowan: Discussion Symposium on Internal Stresses in Metals and Alloys, Monograph and Rept. Series No.5, Institute of Metals, London, 1948, p.451
/63/ B.Reppich, G.Grabenbauer: to be published
/64/ M.Y.Nazmy, R.F.Singer: Scripta Met. 19 (1985) 829
/65/ A.E.Anglin, Jr.: NASA TM-79189, 1979
/66/ J.D.Whittenberger: Met.Trans. 15A (1984) 1753
/67/ K.Monma, H.Suto, H.Oikawa: J.Japan.Inst.Metals 28 (1984) 253
/68/ S.P.Ray, B.D.Sharma: Acta Met. 16 (1968) 981
/69/ R.W.Lund, W.D.Nix: Acta Met. 24 (1976) 469
/70/ J.D.Whittenberger, Met.Trans. 8A (1977) 1155
/71/ O.Ajaja, T.E.Howson, S.Purushothaman, J.K.Tien: Mater.Sci.Eng. 44 (1980) 165
/72/ W.Blum, R.F.Singer: Z.Metallkde. 71 (1980) 312
/73/ E.Arzt, M.F.Ashby, R.A.Verall: Acta Met. 31 (1983) 1977
/74/ J.Lin, O.D.Sherby: Res Mechanica 2 (1981) 251
/75/ R.C.Benn, S.K.Kang, in: M.Gell et al. (eds), Superalloys 1984, Conf. Proc., AIME, 1984, p.321
/76/ R.S.Shewfelt, L.M.Brown: Phil.Mag. 35 (1977) 945
/77/ E.Arzt, M.F.Ashby: Scripta Met. 16 (1982) 1285
/78/ J.H.Hausselt, W.D.Nix: Acta Met. 25 (1977) 1491
/79/ J.Schröder, E.Arzt: Scripta Met. 19 (1985) 1129
/80/ V.C.Nardone, D.E.Matejczyk, J.K.Tien: Acta Met. 32 (1984) 1509
/81/ D.J.Srolovitz, M.J.Luton, R.Petkovic-Luton, D.M.Barnett, W.D.Nix: Acta Met. 32 (1984) 1079
/82/ E.Arzt, D.S.Wilkinson: Acta Met., in press
/83/ E.Arzt, J.Schröder: this volume
/84/ E.Arzt, R.F.Singer, in: M.Gell et al. (eds), Superalloys 1984, Conf. Proc., AIME, 1984, p. 369

/85/ Y.G.Kim and H.F.Merrik, in: J.K.Tien et al. (eds), Superalloys 1980, ASM, Metals Park, Ohio, 1980, p. 551
/86/ W.Hoffelner, R.F.Singer: Met.Trans. 16A (1985) 393
/87/ J.Bressers, E.Arzt: this volume
/88/ D.Hedrich, COST 501, Project D 37, Interim Report, 1984
/89/ J.D.Whittenberger, P.I.Bizon: Int. J.Fatigue (1981) 173
/90/ Ref. /9/, Fig. 7.71 and Fig. 7.72
/91/ Ref. /9/, Fig. 7.75
/92/ Ref. /9/, Fig. 7.71, 7.74, 7.75, 7.76
/93/ B.Jahnke, A.R.Nicoll, in: Ref /10/, p. 190
/94/ T.K.Glasgow, G.J.Santoro, in: J.S.Benjamin, Frontiers of High Temperature Materials, Conf. Proc., IncoMAP New York City, 1981, p. 23
/95/ M.A.Gedwill, T.K.Glasgow, R.S.Levine: Thin Solid Films 95 (1982) 65
/96/ F.R.Wermuth, A.R.Stetson: NASA CR-120852, 1971
/97/ P.Huber: COST 501, Project CH 7, Interim Report 1985
/98/ A.K.Telama, K.T.Torkkell, T.A.Mäntylä, P.O.Kettunen: this volume